frontiers in
CELLULAR AND INFECTION MICROBIOLOGY

ORIGINAL RESEARCH ARTICLE
published: 09 April 2012
doi: 10.3389/fcimb.2012.00048

Evolutionary blueprint for host- and niche-adaptation in *Staphylococcus aureus* clonal complex CC30

Martin J. McGavin[1]*, Benjamin Arsic[1] and Nicholas N. Nickerson[2]

[1] *Department of Microbiology, Schulich School of Medicine and Dentistry, Siebens Drake Research Institute and Centre for Human Immunology, University of Western Ontario, London, ON, Canada*
[2] *Department of Molecular and Cellular Biology, University of Guelph, Guelph, ON, Canada*

Edited by:
David Heinrichs, University of Western Ontario, Canada

Reviewed by:
Steven Gill, University of Rochester School of Medicine and Dentistry, USA
Jodi A. Lindsay, St George's University of London, UK

****Correspondence:***
Martin J. McGavin, Department of Microbiology, Schulich School of Medicine and Dentistry, and Centre for Human Immunology, Western University, London, ON N6A 5C1, Canada.
e-mail: martin.mcgavin@schulich.uwo.ca

Staphylococcus aureus clonal complex CC30 has caused infectious epidemics for more than 60 years, and, therefore, provides a model system to evaluate how evolution has influenced the disease potential of closely related strains. In previous multiple genome comparisons, phylogenetic analyses established three major branches that evolved from a common ancestor. Clade 1, comprised of historic pandemic phage type 80/81 methicillin susceptible *S. aureus* (MSSA), and Clade 2 comprised of contemporary community acquired methicillin resistant *S. aureus* (CA-MRSA) were hyper-virulent in murine infection models. Conversely, Clade 3 strains comprised of contemporary hospital associated MRSA (HA-MRSA) and clinical MSSA exhibited attenuated virulence, due to common single nucleotide polymorphisms (SNP's) that abrogate production of α-hemolysin Hla, and interfere with signaling of the accessory gene regulator *agr*. We have now completed additional *in silico* genome comparisons of 15 additional CC30 genomes in the public domain, to assess the hypothesis that Clade 3 has evolved to favor niche adaptation. In addition to SNP's that influence *agr* and *hla*, other common traits of Clade 3 include tryptophan auxotrophy due to a di-nucleotide deletion within *trpD*, a premature stop codon within *isdH* encoding an immunogenic cell surface protein involved in iron acquisition, loss of a genomic toxin–antitoxin (TA) addiction module, acquisition of *S. aureus* pathogenicity islands SaPI4, and SaPI2 encoding toxic shock syndrome toxin *tst*, and increased copy number of insertion sequence ISSau2, which appears to target transcription terminators. Compared to other Clade 3 MSSA, *S. aureus* MN8, which is associated with Staphylococcal toxic shock syndrome, exhibited a unique ISSau2 insertion, and enhanced production of toxic shock syndrome toxin encoded by SaPI2. Cumulatively, our data support the notion that Clade 3 strains are following an evolutionary blueprint toward niche-adaptation.

Keywords: *Staphylococcus aureus*, evolution, pseudogene, pathogenicity island, insertion sequence, toxin-antitoxin addiction module, pathoadaptation, virulence

INTRODUCTION

Society has become imbued with the Superbug label to define strains of antibiotic resistant bacteria that cause hospital-associated outbreaks of infection (Foster, 2004; Abbott, 2005; Brazier, 2008; Guo et al., 2011). This term, denoting the sudden emergence and spread of new antibiotic resistant strains, could also be applied to an historic global pandemic caused by a penicillin-resistant *S. aureus* clone known as phage type PT80/81, which emerged in Australia, Great Britain, and North America in the early 1950's (Rountree and Beard, 1958; Williams et al., 1959; Wormald, 1961; Tanimoto, 1962). The initial outbreaks occurred in hospitals, especially among newborns and nursing mothers, but quickly spread to the wider community, causing unusually severe invasive skin infections, and fatal sepsis or necrotizing pneumonia in young and healthy individuals (Hassall and Rountree, 1959). Although the pandemic dissipated after 10 years (∼1953–1963), concomitant with the introduction of methicillin, genetically related contemporary strains are prominent in both the community and health-care settings. These consist of clinical methicillin susceptible *S. aureus* (MSSA), the epidemic EMRSA-16 lineage of hospital associated MRSA (HA-MRSA) which has the Type II Staphylococcal cassette chromosome SCC*mec* element, and the hyper-virulent Southwest Pacific (SWP) clone of community associated MRSA (CA-MRSA) which, like other unrelated CA-MRSA, has Type IV SCC*mec*. All of these strains belong to clonal complex CC30 as determined by multi locus sequence typing (MLST) analysis (Robinson et al., 2005).

To better understand the evolutionary development of CC30, we recently employed comparative genome sequencing to evaluate nine CC30 strains (DeLeo et al., 2011), including the reference genome of MRSA 252, representing the EMRSA-16 clone of HA-MRSA (Holden et al., 2004; Lindsay and Holden, 2004). Phylogenetic analyses based on a contiguous 1.4 Mb region of each genome, or with concatenated nucleotide segments, supported the existence of three major branches that evolved from a common ancestor. Clade I consists of the historic PT80/81

pandemic. This clonal type is typically ST30*spa*43, as determined by MLST and staphylococcal Protein A (*spa*) gene typing, and possesses the Panton Valentin Leukotoxin (PVL), that is also characteristic of contemporary CA-MRSA, including the SWP clone, which is ST30*spa*19 and comprises Clade 2. Although temporally separated by nearly 50 years, Clades 1 and 2 share a number of common traits, which in addition to PVL, include abundant production of α-hemolysin Hla, elevated transcription of RNAIII encoded by the accessory gene regulator *agr* locus, and a hypervirulent trait in murine infection models (DeLeo et al., 2011).

Clade 3 is comprised of the EMRSA-16 clone of HA-MRSA, which is typically ST36*spa*16, and contemporary clinical methicillin susceptible *S. aureus*, which are often ST30*spa*33. Although Clade 3 strains exhibited attenuated virulence in murine infection models relative to Clades 1 and 2, these are still associated with a high burden of disease. EMRSA-16, which is known in the United States as USA200, has become one of the most successful HA-MRSA clones (Cox et al., 1995; Enright et al., 2000; Johnson et al., 2001; McDougal et al., 2003; Seybold et al., 2006; Fowler et al., 2007). Others defined an association of CC30 MSSA, frequently ST30*spa33*, with bacteremia, infective endocarditis, and osteomyelitis (Cassat et al., 2005; Fowler et al., 2007; Nienaber et al., 2011). Staphylococcal toxic shock syndrome, which emerged in the late 1970's (Altemeier et al., 1981), is also associated with CC30, and the *tst* gene encoding toxic shock syndrome toxin has a strong clonal association with CC30 nasal carriage and bacteremia isolates (Holtfreter et al., 2007). MSSA that resemble the EMRSA-16 clone were also commonly associated with asymptomatic nasal carriage in the United States (Kuehnert et al., 2006), and other studies concur that CC30 is a major clonal complex associated with nasal carriage (Feil et al., 2003; Melles et al., 2004; Kuehnert et al., 2006; Fowler et al., 2007; Ko et al., 2008; Melles et al., 2008). Therefore, although Clade 3 exhibits attenuated virulence in murine infection models, we proposed that the high burden of disease associated with these hospital associated strains could be due to the high incidence of colonization, affording more opportunity to cause infection.

Several observations support the contention that Clade 3 evolved to favor enhanced colonization, at the expense of attenuated virulence. Foremost, the genome of MRSA 252 has the highest content of pseudogenes compared to other *S. aureus* genomes (Holden et al., 2004), and gene decay is a major force in niche-adaptation of microbial pathogens (Moran and Plague, 2004). Most notable among the pseudogenes was a CAG to TAG transition at Gln_{113} of *hla* encoding α-hemolysin (Hla), which is a major lethal virulence factor of CA-MRSA (Bubeck Wardenburg et al., 2007). This mutation, which creates a premature stop codon, is broadly disseminated in Clade 3, including HA-MRSA and clinical MSSA (DeLeo et al., 2011). Clade 3 strains also possessed a single nucleotide polymorphism (SNP) in *agrC* of the accessory gene regulator *agr* locus, causing a Gly_{55} >Arg change in the AgrC sensor protein, leading to attenuated transcription of the RNAIII product that is needed to produce secreted virulence factors (DeLeo et al., 2011). Consequently, attenuated transcription of *agr*, and inability to produce Hla contribute to the attenuated virulence of Clade 3.

Other defining traits of genomes that are in transition toward niche adaptation include acquisition of mobile genetic elements, and amplification of insertion sequence (IS) elements (Moran and Plague, 2004). However, a common limitation of conducting multiple genome comparisons by mapping short sequence reads from multiple strains on to a known reference genome is that it may not detect large insertions or deletions that differentiate one or more strains from the reference genome. Accordingly, although *tst* encoding toxic shock syndrome toxin is associated with different *S. aureus* pathogenicity island (SaPI) structures, and has a strong clonal association with CC30, *tst* was not present in the MRSA 252 reference genome, and we failed to identify the relevant SaPI through multiple genome comparisons. Herein, we present a detailed analysis of the hypothesis that Clade 3 strains have evolved in favor of niche adaptation, by conducting *in silico* comparisons of 15 additional CC30 genomes that are available in the public domain. Our analysis of pseudogenes, SaPI and IS elements, and gene deletion events, support the hypothesis that Clade 3 is following an evolutionary blueprint towards host- and niche-adaptation.

MATERIALS AND METHODS

BACTERIAL STRAINS AND GROWTH CONDITIONS

A description of CC30 strains that were used in this study for analysis of secreted proteins and PCR assays is provided in **Table 1**. In addition, *S. aureus* RN4220 was obtained from Richard Novick (Novick, 1991). When needed for production of secreted proteins, cultures were grown overnight in tryptic soy broth (TSB; Difco) supplemented with 0.25% glucose, then sub-cultured into 25 ml of fresh TSB in a 125 ml Erlenmeyer flask to an initial optical density of 0.01 ($OD_{600} = 0.01$), and grown for 18 h at 37°C on an orbital shaker at 150 rpm. To assess *yefM-yoeB* addiction module function, cells were grown on brain heart infusion (BHI) agar supplemented with 10 μg/ml erythromycin for plasmid maintenance, and 5 μm cadmium where indicated for induction of the P_{cad} promoter.

GENOME COMPARISONS

Table 2 provides information on 19 CC30 strains for which genome sequence data are available in the public domain. Of these, MRSA 252 (Holden et al., 2004) was used as a reference genome for SNP analysis of multiple CC30 genomes (DeLeo et al., 2011), which in addition to MRSA 252 included three other strains listed in **Table 2**; M1015, WBG10049, and MN8. Of the genomes referred to in **Table 2**, those of TCH60 and MRSA 252 are assembled as a single nucleotide sequence, and all others are in assembly phase. Sequence coverage ranged from 10.5× (WW2703/97) to 36× (MN8). Unpublished genome data from strain UAMS-1 was provided by Dr.'s Mark Smeltzer and Jacques Schrenzel. The Basic Local Alignment Search Tool (BLAST) was used to query these genomes with segments of the annotated genome of MRSA 252 (Holden et al., 2004). Query segments were selected on the basis of SNP's, indels, or mobile genetic elements previously noted in the genome of MRSA 252, that were of discriminatory value in assigning evolutionary variants of CC30 (DeLeo et al., 2011). Genomes were also queried with the integrase (*int*) gene of known *S. aureus* pathogenicity islands (SaPI),

Table 1 | Strains used in this study.

Strain	Description	Clade[a]	Year	MLST	Spa type[b]	Source/Reference
ATCC 12598; Cowan	Pre-pandemic; septic arthritis	ND	1935	ST30	99/t076	ATCC
NRS204; Florey	Pre-pandemic	ND	1940	ST30	251/t318	Barry Kreiswirth
ATCC 25923; Seattle 1945	Pre-pandemic	ND	1945	ST243[c]	43/t021	ATCC
M809	PT80/81 pandemic	1	1961	ST30	43/t021	Robinson et al., 2005
M1015	PT80/81 pandemic	1	1962	ST30	43/t021	Robinson et al., 2005
WBG10049	CA-MRSA; Southwest Pacific Clone	2	1999	ST30	19/t019	Robinson et al., 2005
MN8	Contemporary MSSA; menstrual toxic shock	3	1980	ST30	33/t012	Schlievert and Blomster, 1983
L516	Contemporary MSSA; infective endocarditis	3	1994	ST30	33/t012	Lindsay Nicolle, University of Manitoba
L528	Contemporary MSSA; bacteremia	3	1994	ST30	33/t012	Lindsay Nicolle, University of Manitoba
UAMS-1	Contemporary MSSA; osteomyelitis	3	1995	ST30	33/t012	Gillaspy et al., 1995
PM7	HA-MRSA; EMRSA-16	3	2002	ST36[c]	16/t018	Moore and Lindsay, 2002
PM64	HA-MRSA; EMRSA-16	3	2002	ST36[c]	16/t018	Moore and Lindsay, 2002

[a] *ND, not determined.*

[b] *Provided in both Kreiswirth [Shopsin et al. (1999)] and Ridom (spa.ridom.de) nomenclature.*

[c] *Single-locus MLST variants of ST30.*

to identify contigs that contained SaPI structures. Genome segments containing SaPI's and other mobile genetic elements or genes of interest were analyzed using MacVector version 7.2.3 software (Accelerys).

PCR was employed to assess presence or absence of two unique ISSau2 insertions in different strains. One insertion adjacent to the *saeRS* regulatory locus was detected with primers SAR0758_For 5′-CAATATCGAACGCCACTTGAGC-3′, and SAR0757_Rev 5′-CAGCTATGATTGCAGGTTACCAGC-3′. Another insertion adjacent to the 5S-rRNA-3 site (**Figure 1**) was detected with primers SAR2148_For 5′-TTTCCCTCAACGTCCAGGTGC-3′ and 5S-rRNA-Rev 5′-GCCGAACACAGAAGTTAAGCTCC-3′. PCR was conducted with Roche AmpliTaq Gold DNA polymerase.

ANALYSIS OF SECRETED PROTEINS

Isolates representing different CC30 genotypes were cultured for 18 h in TSB, after which proteins in the cell-free culture supernatant were precipitated with trichloroacetic acid, and subjected to SDS-PAGE as described previously (Nickerson et al., 2010). For detection of Hla, Western blot assays were conducted with PVDF membrane (Pall Corporation), and rabbit anti-Staphylococcal α-toxin primary antibody (Sigma). The secondary antibody was donkey anti-rabbit IgG IR800 conjugate (Rockland Immunochemicals Inc.), and blots were visualized on an Odyssey Infrared Imager from LiCor Biosciences.

Identification of Coomassie-Blue stained proteins was conducted at the London Regional Proteomics Centre at the University of Western Ontario. Protein bands were excised using an Ettan^{TM} Spot Picker, and processed for mass spectrometry using a Waters MASSPrep Automated Digestor as described (Gyenis et al., 2011). Processed samples were spotted on MALDI plates and analyzed on an Applied Biosystems 4700 Proteomics Analyzer. Data were acquired and processed using 4000 Series Explorer and Data Explorer (Applied Biosystems), and the peptide fingerprints were compared to the NCBInr database for Gram-positive bacteria, using the MASCOT search engine.

CLONING AND EXPRESSION OF *yefM-YoeB* TOXIN–ANTITOXIN TA-MODULE

Gene segments were amplified by PCR, and cloned in pCN51 (Charpentier et al., 2004), for expression of the *yefM-yoeB* antitoxin-toxin genes together, or *yoeB* toxin on its own, from the cadmium inducible P_{cad} promoter. PCR was conducted using template DNA from *S. aureus* strain M1015, with primers YefM_For 5′-cgc***ggatcc***gttaactaattaaCAA*AGGAGG* GTTTATATGATTATC-3′, and YoeB_Rev 5′-tt***ggcgcgcc***TTAATC ATAATGTGACCATGCCG-3′, generating a 538 nt product containing *yefM-yoeB*. The lower case nucleotides incorporate *BamHI* (***ggatcc***) or *AscI* (***ggcgcgcc***) restriction sites, and in YefM_For also add TAA stop codons in all three open reading frames prior to the *AGGAGG* ribosome binding site of *yefM*. For *yoeB*, primers YoeB_For 5′-cgc***ggatcc***gttaactaattaa *caaaggagggtttat*ATGAGCAATTACACGGTTAAG-3′, and YoeB_Rev were used to generate a 266 nt product. The underlined lower case nucleotides in YoeB_For incorporate the ribosome binding site that precedes *yefM*, such that both constructs have identical P_{cad} promoter and translation initiation signals. PCR products were digested with *BamHI* and *AscI*, and ligated into pCN51 that had been digested with the same enzymes. The ligated plasmids were electroporated into restriction deficient *S. aureus* RN4220, and transformants were selected for growth on BHI agar containing 10 μg/ml erythromycin for maintenance of pCN51.

RESULTS

CC30 STRAINS ARE DIFFERENTIATED BY CONSERVED PSEUDOGENES

Our present analysis reveals that previously emphasized defects in *hla* and *agrC* (DeLeo et al., 2011), co-associate with lesions in *isdH* and *trpD* (**Table 2**). IsdH is a cell surface protein that is

Table 2 | Summary of CC30 strains and genotypic data.

CLADE:													ISSau2[e]				
Isolate[a]	**PRJNA**[b]	**Year**	**Country**	**Genotype**	**SCC*mec***	**PVL**[d]	***agrC***	***hla***	***isdH***	***trpG***	**TA-module**	**SaPI**	***trpS***	***rRNA-3***	***rplQ***	***sbcC***[f]	***saeRS***
CLADE 1:																	
55/2053	55909	1955	England	ST30*spa*43	MSSA	P	Gly_{55}	CAG_{Gln}	CAA_{Gln}	6TG	P	SaPI1	P		A	A	A
58–424	47005	1958	GA, USA	ST30*spa*43	MSSA	P	Gly_{55}	CAG_{Gln}	CAA_{Gln}	6TG	P	SaPI1	P	P	A	A	A
E1410	55915	1962	Denmark	ST30*spa*43	MSSA	A	Gly_{55}	CAG_{Gln}	CAA_{Gln}	6TG	P	SaPI1	P		A	A	A
M1015[c]	47009	1962	Australia	ST30*spa*43	MSSA	P	Gly_{55}	CAG_{Gln}	CAA_{Gln}	6TG	P	SaPI1	P	P	A	A	A
M876	55917	1961	Australia	ST30*spa*43	MSSA	P	Gly_{55}	CAG_{Gln}	CAA_{Gln}	6TG							
M809	47007	1961	Australia	ST431*spa*43	MSSA	P	Gly_{55}	CAG_{Gln}	CAA_{Gln}	6TG	P	SaPI1	P	P	A	A	A
M899	42993	1961	Australia	ST30*spa*43	MSSA	P	Gly_{55}	CAG_{Gln}	CAA_{Gln}	6TG	P	SaPI1	P		A	A	A
65–1322	55911	1965	WV, USA	ST30*spa*43	MSSA	P	Gly_{55}	CAG_{Gln}	CAA_{Gln}	6TG	P	SaPI1	P		A	A	A
68–397	55913	1968	TX, USA	ST30	MSSA	P	Gly_{55}	CAG_{Gln}	CAA_{Gln}	6TG	P	SaPI1	P		A	A	A
C101	43001	1997	England	ST30*spa*43	MSSA	A	Gly_{55}	CAG_{Gln}	CAA_{Gln}	6TG	P	SaPI1	P		A	A	A
CLADE 2:																	
WBG10049[c]	42991	1999	Australia	ST30*spa*19	IV	P	Gly_{55}	CAG_{Gln}	CAA_{Gln}	6TG	P	SaPI1	P	P	A	A	A
TCH60	CP002110		TX, USA	ST30*spa*19	IV	P	Gly_{55}	CAG_{Gln}	CAA_{Gln}	6TG	P	SaPI1	P	P	A	A	A
CLADE 3:																	
MN8[c]	59529	1980	MN, USA	ST30*spa*33	MSSA	A	Arg_{55}	TAG*	TAA*	5TG	A	SaPI2, SaPI4	P	A	P	A	P
UAMS-1		1995	AR, USA	ST30*spa*33	MSSA	A	Arg_{55}	TAG*	TAA*	5TG	A	SaPI2, SaPI4	P	A	P	A	A
Btn1260	42987	1999	England	ST30*spa*33	MSSA	A	Arg_{55}	TAG*	TAA*	5TG	A	SaPI2, SaPI4	P	A	P	A	A
MRSA 252[c]	57839	1990's	England	ST36*spa*16	II	A	Arg_{55}	TAG*	TAA*	5TG	A	SaPI4	P	A	P	P	A
EMRSA-16	48295	1990's	England	ST36*spa*16	II	A	Arg_{55}	TAG*	TAA*	5TG	A	SaPI2, SaPI4	P	A	P	P	A
A017934/97	43393	1997	Sweden	ST30*spa*43	IV	A	Arg_{55}	TAG*	TAA*	5TG	A	SaPI2, SaPI4	P	A	P	A	A
WW2703/97	42989	1997	Germany	ST30*spa*16	IV	A	Arg_{55}	TAG*	TAA*	5TG	A	SaPI4	P	A	P	A	A

[a] *Data for year, country, MLST, spa, SCCmec and PVL derived from [Robinson et al. (2005)], with exception of TCH60, MN8, and UAMS-1.*

[b] *Public domain whole genome sequencing project nucleic acid sequence accession number.*

[c] *Included in genome comparisons conducted by SOLiD 3 sequencing and SNP analysis [DeLeo et al. (2011)].*

[d] *Defined as present (P) or absent (A), as also for toxin-antitoxin module (TA) and SaPI elements.*

[e] *ISSau2 insertion sites defined in **Figures 1** and **3**.*

[f] *Same distribution profile for ISSau2 insertions at sbcC, rRNA-1 and rRNA-2.*

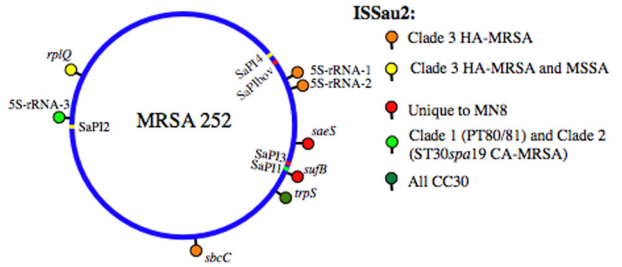

FIGURE 1 | SaPI and ISSau2 distribution in CC30. The location of each element is mapped on the reference genome of MRSA 252 [Holden et al. (2004)]. SaPIs are indicated by colored bars, on the circular blue genome, and are labeled on the interior of the circular genome. SaPI2 and SaPI4 (yellow) are unique to Clade 3. SaPI1 (light green) is present in PT80/81 (Clade 1) and ST30*spa19* CA-MRSA (Clade 2). SaPI3 and SaPIbov (red) are not in CC30, but their location is shown for reference, based on location of *attS* sites. ISSau2 insertions, indicated by colored lollipops above the circular genome, are named after the gene that is adjacent to each insertion. Three different 16S-23S-5S-rRNA loci are abbreviated as 5S-rRNA-1, 5S-rRNA-2, and 5S-rRNA-3.

highly expressed under iron-limiting conditions, and immunization with IsdH protects against *S. aureus* nasal carriage and bovine mastitis (Clarke et al., 2006; Pilpa et al., 2006; Ster et al., 2010). In EMRSA-16 and ST30*spa33* MSSA, *isdH* has a SNP that converts CAA_{Gln} into a TAA stop codon (**Table 2**). An observation that many TSST producing strains are auxotrophic for tryptophan (Kreiswirth et al., 1989; Leung et al., 1993) is accounted for by a TG deletion in a 6×TG segment of *trpD*, in the *trpEGDCFBA* locus. Therefore, *agrC*, *hla*, *isdH*, and *trpD* are defective in contemporary MSSA and EMRSA-16 comprising Clade 3, but are functional in PT80/81 and ST30*spa19* CA-MRSA comprising Clades 1 and 2 (**Table 2**). These latter strains also have PVL, which together with Type IV *SCCmec* is a trait that Clade 2 CA-MRSA shares with other unrelated CA-MRSA, such as USA300 and USA400. Other CC30 strains A01734/94 (ST30*spa43*), and WW2703/97 (ST30*spa16*) in Clade 3 are defined as CA-MRSA due to Type IV *SCCmec*, but they lack PVL, and have the "pseudogene package" (*agrC*, *hla*, *isdH*, and *trpD*) (**Table 2**), which we refer to as a niche-adapted trait.

S. aureus PATHOGENICITY ISLAND (SaPI) CONTENT

Figure 1 summarizes the distribution of insertion sequence ISSau2, and SaPI's in CC30. Irrespective of gene composition or genetic background, a SaPI is defined by a specific integrase *int* that recognizes an *attS* site (Lindsay and Holden, 2004; Novick and Subedi, 2007). Our analysis reveals that the *attS* sites are always located at the 3′-end of a gene, often in association with an operon, and these structures are illustrated in **Figure 2**. As noted previously (DeLeo et al., 2011), SaPI-4 differentiates Clade 3 from Clades 1 and 2. The *attS* of SaPI4 is at the 3′-end of the *rpsF-ssb-rpsR* operon, encoding ribosomal protein S6, a single stranded RNA binding protein, and ribosomal protein S18 (**Figure 2A**). SaPI4 does not have any known virulence factors, but SAR0385 encodes a protein with a signal peptide, identical to ORF011 of *S. aureus* phage ϕ1028 (Kwan et al., 2005). Outside of CC30, SaPI4 is restricted to ovine adapted *S. aureus* strains 011 and 046 (Le Marechal et al., 2011), which have an ortholog of SAR0385 (**Figure 2A**). In bovine adapted *S. aureus* ET3-1 (Herron-Olson et al., 2007), an ortholog of SAR0385 is on SaPIbov, where it is flanked by *tst*, *sec*, and *sel* encoding superantigen toxins (**Figure 2A**). The *attS* of SaPIbov spans the 3′- end of the *xpt-pbuX-guaB-guaA* operon, encoding genes for transport and metabolism of purine nucleotides. The *rpsR* and *guaA* genes, which contain the *attS* sites for SaPI4 and SaPIbov, respectively, are in close proximity (**Figure 1**), and segments of SaPIbov exhibit high similarity to ϕ1028, and SaPI4 (**Figure 2A**), but there are no genomes that have both SaPI's.

In CC30, the toxic shock syndrome toxin *tst* is on SaPI2, where *attS* spans the 3′-end of *groES-groEL* (**Figure 2B**). In CC30, *tst* is the only toxin on SaPI2, but in unrelated HA-MRSA strains N315 and Mu50 (Kuroda et al., 2001), SaPI2 has additional superantigen toxins *sec* and *sel* (**Figure 2B**). In another non-CC30 strain, *tst* co-associates with *sec* and *sel* in SaPI3 (Li et al., 2011), where *att*S overlaps with the 3′-end of *rnr-smpB-ssrA* (**Figure 2C**). This operon encodes a ribonuclease (*rnr*), a non-translated RNA *ssrA*, and its cognate binding protein *smpB*. In the USA400 CA-MRSA, SaPI3 has superantigen toxins *sec* and *sel*, but not *tst*. However, CC30 genomes do not have SaPI3.

The first SaPI identified in *S. aureus* was SaPI1 in strain RN4282 (Lindsay et al., 1998; Ruzin et al., 2001), which has superantigen enterotoxins *sek* and *seq* at the 5′-end, and *tst* at the 3′-end (**Figure 2D**). The genome of RN4282 was not sequenced, but the flanking *attS* sequences of SaPI1 establish the integration site at the 3′-end of *metNPQ*, encoding a putative methionine transporter. Similar SaPI1 structures are in *S. aureus* COL and USA300, although these lack *tst* (**Figure 2D**). In CC30 SaPI1 is present in Clade 1 and 2 strains (**Table 2**), but does not have any obvious virulence factors. Similar SaPI1 structures that lack known virulence factors are in *S. aureus* ED98 (Lowder et al., 2009), which has undergone a recent evolutionary transition from human to poultry host, and in bovine adapted strain LGA251 (Garcia-Alvarez et al., 2011). In summary, although *tst* has been identified on SaPI1, SaPI2, SaPI3, and SaPIbov, depending on the genetic background, our data indicate that in CC30 it exclusively resides on SaPI2, where unlike other SaPI2 structures, *tst* does not co-associate with other superantigen toxins.

ANALYSIS OF ISSau2 CONTENT

CC30 strains are distinguished by their profiles of ISSau2 (**Figure 1**), which is a member of the IS3 family (www-is.biotoul.fr/is.html). In *E. coli*, IS3 is flanked by imperfect inverted 39 nucleotide repeats with terminal 5′-TG and CA-3′ dinucleotides, and has two overlapping reading frames *orfA* and *orfB*, which when produced by default, prohibit transposition (Timmerman and Tu, 1985; Sekine et al., 1997). A –1 translational frame-shift within a poly-A tract in the region of overlap between *orfA* and *orfB* produces a single protein that catalyzes transposition (Prere et al., 1990; Sekine et al., 1994), with duplication of a three base pair target site (Sekine et al., 1994, 1997). ISSau2 has similar features (**Figure 3A**), and targets inverted repeats (**Figures 3B–G**), likely comprising *rho*-independent transcription terminators. An ancestral insertion

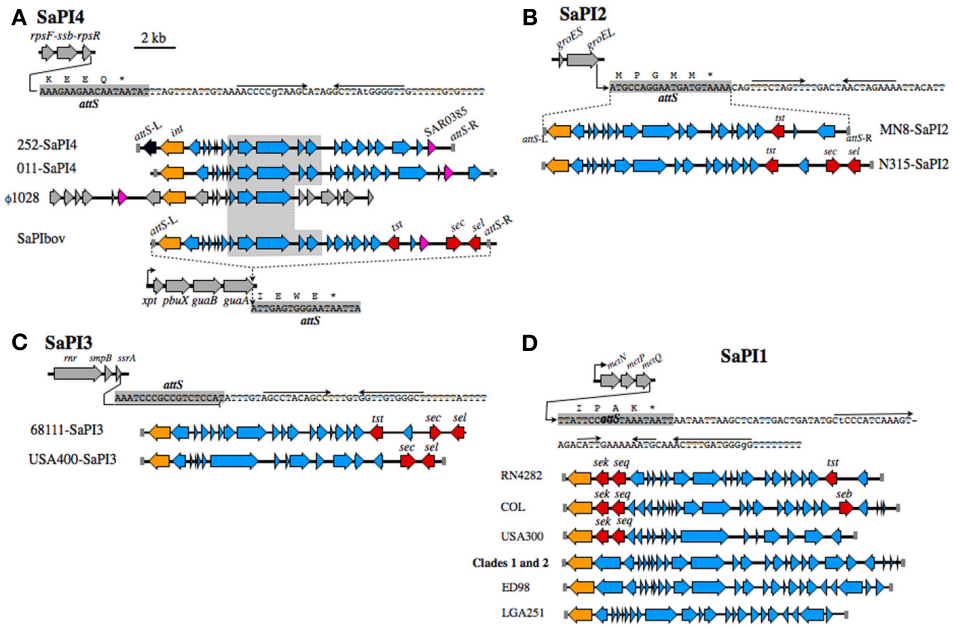

FIGURE 2 | SaPI structures and insertion sites. (A) SaPI4, with an illustration of the *rpsF-ssb-rpsR* operon, and nucleotide sequence extending from the 3′-end of *rpsR*. The *attS* of SaPI4 shaded gray, overlaps the 3′-end of the *rpsR* open reading frame, and letters above the sequence correspond to the C-terminus of RpsR protein. Arrows above the nucleotide sequence indicate inverted repeats, likely comprising a transcriptional terminator. Illustrations below the sequence compare SaPI4 of *S. aureus* MRSA 252 with that of ovine adapted strain 011. The duplicated left and right *attS* sequences are shaded gray, *int* genes are colored orange, while SAR0385 and orthologous genes, encoding a putative secreted protein, are magenta. A central outlined and shaded segment of SaPI4 is highly conserved in *S. aureus* phage ϕ1028, and SaPIbov of bovine adapted *S. aureus* ET3-1. Genes in SaPIbov encoding superantigen toxins are shaded red. The *int* of SaPIbov is shaded orange to emphasize function, although each SaPI family has a distinct *int* and *attS*. Structures of SaPI2 **(B)**, SaPI3 **(C)**, SaPI1 **(D)**, and their genomic insertion sites. Features are labeled as in **A**. SaPI2 of ST30*spa*33 strain MN8 **(B)**, is compared to SaPI2 of a non-related MRSA strain N315. SaPI3 **(C)** is not present in CC30. Structures shown are from strain USA400 [Baba et al. (2002)], which is a CA-MRSA, and strain 68111, which is a triple locus MLST variant of ST30 [Li et al. (2011)]. A clonal complex is comprised of isolates that differ from the ancestral sequence type (ST) at no more than two of seven MLST alleles. Therefore, *S. aureus* 68111 is distantly related to ST30, but is not within CC30. **(D)** shows SaPI1 structures from different strains, in comparison to SaPI1 in Clade 1 PT80/81 strains, and Clade 2 ST30*spa*19 CA-MRSA.

common to CC30 genomes occurs in the intergenic segment separating *trpS* from the *oppAFDBC* oligopeptide permease operon (**Figure 3B**). ST30*spa19* CA-MRSA and PT80/81 have one additional insertion, adjacent to a 16S-23S-5S rRNA operon (**Figures 1** and **3C**). Two other 16S-23S-5S-rRNA loci are targeted in EMRSA-16, which has a third unique insertion adjacent to *sbcDC* (**Figures 1**, and **3D,F**). A fourth insertion adjacent to *rplQ* is also present in ST30*spa33* MSSA (**Figures 1** and **3E**), including strain MN8, a prototypic menstrual toxic shock strain (Schlievert and Blomster, 1983). MN8 is distinguished from other ST30*spa33* strains by two unique insertions (**Figure 1**), one of which is adjacent to *saeRS* (**Figure 3G**), encoding a two-component sensor signal transduction system that is a major regulator of virulence.

Outside of CC30, ISSau2 is restricted to animal adapted *S. aureus*. Ovine adapted ED133 has seven copies (Guinane et al., 2010), bovine strain LGA251 has three (Garcia-Alvarez et al., 2011), and porcine adapted ST398 has one (Schijffelen et al., 2010). The unassembled genomes of ovine strains 011 and 046 also have at least one copy (Le Marechal et al., 2011). In these animal adapted strains, the integration sites for ISSau2 are mutually exclusive of those in CC30.

LOSS OF A TOXIN–ANTITOXIN ADDICTION MODULE IN CC30 EVOLUTION

Toxin-antitoxin (TA) modules encode a stable bactericidal or bacteriostatic toxin, and an unstable antitoxin that forms an inhibitory complex with the toxin. These were first termed addiction modules when discovered on plasmids, since loss of the plasmid during cell division leads to rapid degradation of the unstable antitoxin, followed by activation of the toxin and death of the daughter cells (Meinhart et al., 2003). Most free-living bacteria also have one or more genomic TA modules (Pandey and Gerdes, 2005). An example in *S. aureus* is *mazEF*, where MazF is an RNA'se that induces cell stasis by degradation of mRNA (Fu et al., 2007), and MazE is the antitoxin. Most other *S. aureus* genomes have another uncharacterized TA module, similar to *yefM-yoeB* in *E. coli*, where YoeB is a stasis-inducing RNA'se and YefM is the antitoxin (Kamada and Hanaoka, 2005). In ST30*spa19* CA-MRSA and PT80/81, *yefM-yoeB* is flanked by *frvX* encoding an M42 metallopeptidase/endoglucanase protein family member, and a predicted glutamate synthase, *gltS* (**Figure 4A**). In MRSA 252, the flanking genes *frvX* (SAR2545) and *gltS* (SAR2547) are present, but not *yefM-yoeB*, and this is also characteristic of contemporary CC30 MSSA. Other genomes with this trait are

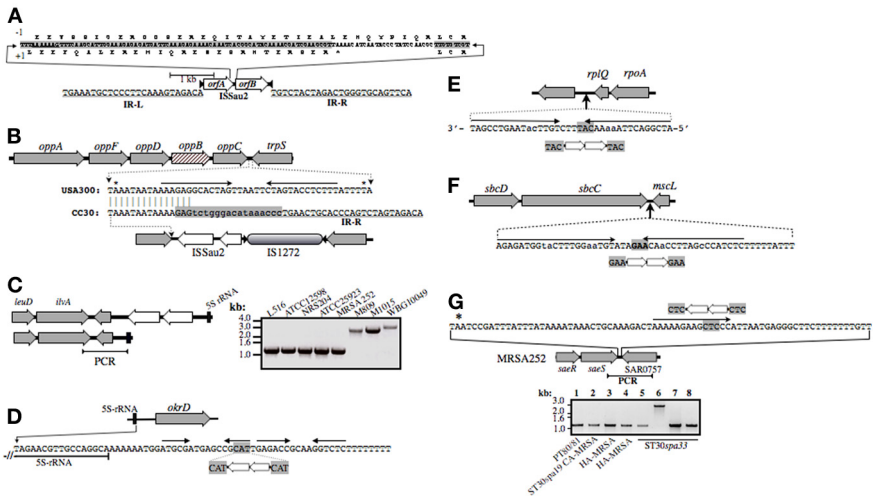

FIGURE 3 | Illustration of ISSau2 (A) and its insertion sites (B–G) in CC30. ISSau2 is comprised of *orfA* and *orfB* **(A)**, flanked by 39 nt inverted repeats IR-L and IR-R, with terminal 5′-TG and 3′-CA dinucleotides **(A)**. The sequence above the illustration spans the 3′-end of *orfA* and 5′-end of *orfB*. The +1 translation of *orfA*, terminating at a stop codon, is shown below the sequence. Above the sequence is a translation that would result from a −1 frame-shift within ***AAAAAAG***. The −1 translation from this point onwards continues throug to the end of *orfB*, and would produce a single 1569 nt trans-frame protein. **(B)** Illustration of *oppAFBDC* and *trpS* genome segment of non-CC30 strain USA300. Beneath this is shown the *oppC-trpS* intergenic sequence of USA300, aligned to that MRSA 252. Asterisks above the USA300 sequence indicate stop codons of *oppC* and *trpS*. Convergent arrows indicate inverted repeats, likely comprising a *rho*-independent transcription terminator stem-loop structure. In all CC30 strains, the left arm of the stem is disrupted by a flanking repeat of IS1272 (shaded gray), which in turn is disrupted by ISSau2. In MRSA 252, *oppB* (cross-hatched) has an in-frame internal deletion that is unique to the EMRSA-16 lineage. **(C)** ISSau2 insertion in the genome of *S. aureus* TCH60 (top), which is ST30*spa19* CA-MRSA (Clade 2), and corresponding segment of MRSA 252 (bottom). PCR with primers spanning the 3′-end of the 5S rRNA and flanking *ilvA* (right panel) reveal that this insertion is in Clade 1 strains (M809, M1015) and another Clade 2 CA-MRSA (WBG10049), but not other CC30, including strains that pre-date the Clade 1 pandemic (ATCC12598, NRS204, ATCC25923). **(D)** ISSau2 insertion adjacent to a 16S-23S-5S rRNA operon, and flanking *okrD* gene, which is unique to Clade 3 HA-MRSA. The sequence below the illustration shows the end of the 5S rRNA transcript, and adjacent *rho*-independent transcriptional terminator, comprised of tandem stem-loops followed by a poly-T segment. ISSau2 disrupts the right arm of the first stem-loop, with duplication of the CAT target site. **(E and F)** show similar disruption of a putative stem-loop structure downstream of *rplQ*, and a likely transcription terminator of the *sbcDC* operon. **(G)** Unique ISSau2 insertion in ST30*spa*33 strain MN8 disrupts stem-loop structure adjacent to *saeRS* regulator. The *saeRS* genome segment of MRSA 252 is shown for reference, and the nucleotide sequence downstream of *saeS* is shown above the illustration. In strain MN8, ISSau2 inserts into the left arm of a putative stem-loop structure, with duplication of the CTC target site. This is confirmed by PCR of a genomic segment spanning *saeS* and adjacent SAR0757, producing a 2.8 kb amplicon in MN8 (Lane 6), and a 1.2 kb product in all other strains including PT80/81 strain M1015 (Lane 1), ST30*spa19* CA-MRSA strain WBG10049 (Lane 2), ST36*spa16* HA-MRSA strains PM7 and PM64 (Lanes 3 and 4), and additional ST30*spa*33 strains UAMS-1 (Lane 5), L516 (Lane 7), and L528 (Lane 8).

restricted to ST398 porcine adapted *S. aureus*, ovine adapted strains 011 and 046, and as yet undefined strains A9635 and 21200.

Although not annotated, *yefM-yoeB* is flanked by long direct repeats LDR-1 and LDR-2 (**Figure 4B**). CC30 genomes that lack *yefM-yoeB* have a single repeat identical to LDR-1, except for two SNP's at the 3′-end that match LDR-2, suggesting that deletion occurred by recombination between LDR-1 and LDR-2. To assess the function of *yoeB*, it was cloned by itself, or paired with *yefM*, in plasmid pCN51 under transcriptional control of P_{cad}. Cells of *S. aureus* RN4220 with either plasmid grew well on BHI agar, but on induction with cadmium, cells with *yoeB* alone did not grow (**Figure 4C**), confirming its function as a toxin, likely through degradation of mRNA to induce cellular stasis.

PRODUCTION OF SECRETED PROTEINS

Clade 3 MSSA (ST30*spa*33) are recovered from a spectrum of conditions, including osteomyelitis (Cassat et al., 2005), infective endocarditis (Nienaber et al., 2011), bacteremia (Xiong et al., 2009), and menstrual toxic shock (Lin et al., 2011). Although these all have the same premature stop codon in *hla*, strains associated with menstrual toxic shock were reported to retain the ability to produce a small amount of Hla (Lin et al., 2011). Further, our data establish that MN8, which is a prototypic menstrual toxic shock strain (Altemeier et al., 1981), is differentiated from other Clade 3 MSSA by unique ISSau2 insertions (**Figures 1**,**3** and **Table 2**), suggesting that it could also have unique phenotypic traits. We, therefore, evaluated production of secreted proteins in the major CC30 clonal types, including PT80/81 (Clade 1), ST30*spa19* CA-MRSA (Clade 2), HA-MRSA (Clade 3), and Clade 3 MSSA recovered from menstrual toxic shock (MN8), osteomyelitis (UAMS-1), infective endocarditis (L516), and bacteremia (L528). Compared to other Clade 3 MSSA, MN8 exhibited more abundant production of secreted proteins (**Figure 5A**), and when compared to UAMS-1 on three separate occasions, it always produced more secreted protein (data not shown). However, irrespective of this difference, Hla was not detected in any of the ST30*spa*33 MSSA in a Western blot (**Figure 5B**).

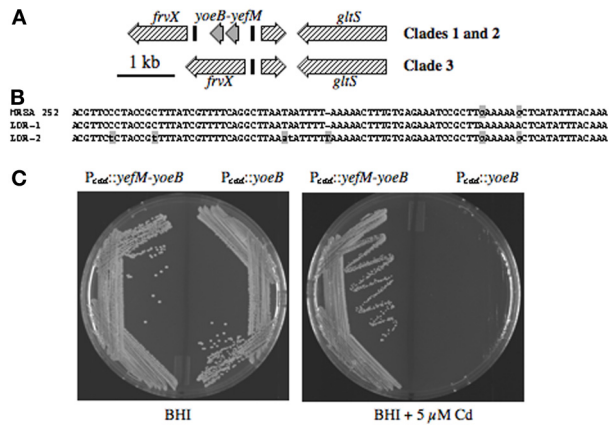

FIGURE 4 | (A) Illustration of *yefM-yoeB* and flanking DNA in CC30. *yefM-yoeB* are flanked by repeats LDR-1 and LDR-2 (black bars) in PT80/81 and ST30*spa19* CA-MRSA, whereas HA-MRSA and contemporary MSSA have only one LDR and lack *yefM-yoeB*. **(B)** Nucleotide sequence of LDR-1 and LDR-2 from strain M1015, and the single LDR of MRSA 252. The lower-case gray shaded nucleotides differentiate LDR-1 and LDR-2. The single LDR of MRSA 252 is a hybrid of LDR-1 and LDR-2, which is suggestive of a recombination event. **(C)** Growth of *S. aureus* RN4220 harboring P_{cad}::*yefM-yoeB* or P_{cad}::*yoeB*, on BHI agar, or BHI supplemented with 5 μM cadmium, to induce P_{cad}.

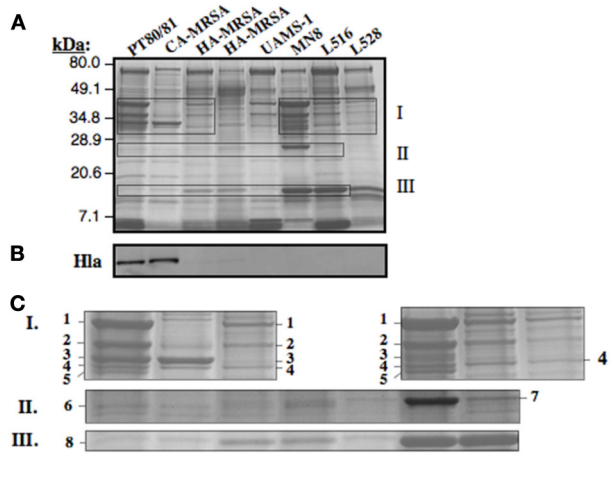

FIGURE 5 | Assessment of CC30 secreted proteins by SDS-PAGE (A) and Western blot for detection of Hla (B). The individual strains are the same as defined in **Figure 3G**. For visualization of secreted proteins by Coomassie Blue staining **(A)**, a total of 3.0 OD_{600} units of cell-free culture supernatant was applied to each lane, while 0.02 OD units was applied in **Figure 3B**. Zones I, II, and III as outlined in the SDS-PAGE gel **(A)** are enlarged in **Figure 3C**. The numbered protein bands were excised from the gel, followed by trypsin digestion and mass spectrometry. The identity of proteins in each band is provided in **Table 3**.

Proteins from zones I, II, and III on the SDS-PAGE (**Figure 5A**) were selected for trypsin digestion and mass spectrometry (**Figure 5C** and **Table 3**). HA-MRSA and ST30*spa*33 MSSA secreted toxic shock syndrome toxin TSST (Zone II, band 7), encoded by *tst* on SaPI2, and except for UAMS-1, they also secreted the SAR0385 gene product encoded on SaPI4 (Zone III, band 8). PT80/81 and CA-MRSA produced Hla (Zone I, band 3 and some carry-over in band 4), but Hla was not identified in the co-migrating protein bands from strain MN8. The PT80/81 strain was unique in abundant production of the LukF component of PVL (Zone I, band 2). All strains produced mature glycerol ester hydrolase/lipase (Zone I, band 1), γ-hemolysin components HglC and HglB (band 2 and carry-over in 3), and glycerolphosphoryl diester phosphodiesterase (band 4). With the exception of CA-MRSA, band 4 also contained the HglA component of γ-hemolysin. Therefore, although our data support the contention that Clade 3 MSSA associated with Staphylococcal toxic shock syndrome may be more virulent due to elevated production of secreted proteins, including γ-hemolysin, we found no evidence to support their production of Hla.

DISCUSSION

Gene gain, gene loss, and gene change are major forces in bacterial genome dynamics (Moran and Plague, 2004; Pallen and Wren, 2007), and we have evaluated these processes in *S. aureus* clonal complex CC30. It was previously established that MRSA 252, representing the EMRSA-16 lineage, has the highest content of pseudogenes compared to other *S. aureus* genomes (Holden et al., 2004; Lindsay and Holden, 2004). A bovine adapted strain ET3-1 was a close second, and several of the accumulated pseudogenes would eliminate production of a number of cell surface proteins and iron acquisition pathways (Herron-Olson et al., 2007). Importantly, the most robust examples of gene decay come from recently emerged pathogens that have changed lifestyle, usually to live in a simpler host-associated niche (Moran and Plague, 2004). As summarized in **Table 2**, defining traits of CC30 Clade 3 include (1), a premature stop codon in *hla* encoding α-Hemolysin; (2), a SNP that causes an Gly_{55}>Arg substitution in the AgrC membrane sensor protein, leading to attenuated transcription of the regulatory RNAIII that is needed to produce secreted virulence factors; (3), *isdH* and *trpD* pseudogenes; (4), acquisition of SaPI4, and in most isolates also SaPI2, which possesses the *tst* gene encoding toxic shock syndrome toxin, and (5), an increase in copy number of ISSau2 relative to Clades 1 and 2. Our analyses have revealed several features that were not previously identified through comparative genome sequencing (DeLeo et al., 2011). These include the presence of SaPII and a functional TA genomic addiction module in Clades 1 and 2, the identification of SaPI2 in Clade 3, and the occurrence of unique ISSau2 insertions in each of the three major Clades. Cumulatively, these findings are concordant with niche adaptation in CC30 Clade 3.

It has long been known that 80% of TSST producing *S. aureus* strains are auxotrophic for tryptophan (Chu et al., 1985; Leung et al., 1993), which we now attribute to a TG deletion in *trpD*. It is believed that amino acid auxotrophy contributes to niche adaptation, because auxotrophic bacteria are restricted to a niche where the appropriate amino acid can be obtained. *Lactococcus lactis* recovered from dairy products are auxotrophic for histidine due to frame-shift mutations in *hisC*, *hisG*, and *hisH*, while strains from non-dairy sources are prototrophic (Delorme et al., 1993). *S. aureus* ET3-1, which is a predominant clonal type associated with bovine mastitis, also has a frame-shift mutation in *hisC*

Table 3 | Identity of proteins excised from SDS-PAGE (Figures. 5A and C)

Zone	Band	Strain	Protein	Accession	C.I.
I	1	PT80/81	lipase precursor	gi|49482552	100
		HA-MRSA	lipase precursor	gi|49482552	100
		MN8	lipase precursor	gi|49482552	100
	2	PT80/81	gamma hemolysin HglC component	gi|4948637	99.99
			gamma hemolysin HglB component	gi|477912	99.19
			LukF-PV	gi|9635192	97.83
		CA-MRSA	gamma hemolysin HglC component	gi|4948637	99.99
			gamma hemolysin HglB component	gi|477912	99.94
		HA-MRSA	gamma hemolysin HglC component	gi|4948637	100
			autolysin protein	gi|32968086	100
			gamma hemolysin HglB component	gi|477912	99.96
		MN8	gamma hemolysin HglC component	gi|4948637	100
			gamma hemolysin HglB component	gi|477912	99.98
			autolysin protein	gi|32968086	83.16
	3	PT80/81	alpha hemolysin precursor	gi|15924153	100
		CA-MRSA	alpha hemolysin precursor	gi|15924153	100
		MN8	gamma hemolysin HglC component	gi|49484636	100
			lipase precursor	gi|49482552	76.21
	4	PT80/81	glycerolphosphoryl diester phosphodiesterase	gi|49483119	100
			gamma hemolysin HglA component	gi|49484635	99.88
		CA-MRSA	glycerolphosphoryl diester phosphodiesterase	gi|49483119	99.99
			alpha hemolysin precursor	gi|15924153	99.99
			nucleotidase lipoprotein	gi|49482539	65.61
		MN8	gamma hemolysin HglA component	gi|49484635	100
			glycerolphosphoryl diester phosphodiesterase	gi|49483119	86.31
		L516	glycerolphosphoryl diester phosphodiesterase	gi|49483119	100
			gamma hemolysin HglA component	gi|49484635	100
		L528	glycerolphosphoryl diester phosphodiesterase	gi|49483119	100
			gamma hemolysin chain II (HglA) component	gi|15925409	97.77
	5	PT80/81	lipase precursor	gi|49482552	100
		MN8	lipase precursor	gi|49482552	100
II	6	PT80/81	Staphopain cysteine protease	gi|3891901	96.7
			alkyl hydroperoxidase subunit C	gi|15923371	29.78
		CA-MRSA	alkyl hydroperoxidase subunit C	gi|15923371	91.75
		HA-MRSA	alkyl hydroperoxidase subunit C	gi|15923371	99.8
	7	HA-MRSA	toxic shock syndrome toxin-1	gi|18535666	99.95
		HA-MRSA	toxic shock syndrome toxin-1	gi|18535666	100
		UAMS-1	toxic shock syndrome toxin-1	gi|18535666	100
		MN8	toxic shock syndrome toxin-1	gi|18535666	100
		L516	toxic shock syndrome toxin-1	gi|18535666	100
III	8	PT80/81	hypothetical protein SAR0622	gi|49482843	99.93
		CA-MRSA	hypothetical protein SAR0622	gi|49482843	99.89
		HA-MRSA	hypothetical protein SAR0385	gi|49482618	98.66
		UAMS-1	hypothetical protein SAR0622	gi|49482843	100
		MN8	hypothetical protein SAR0385	gi|49482618	98.66

(SAB2553), which does not occur in other *S. aureus* genomes. The *trpD* gene, which has a TG insertion in CC30 Clade 3, is part of the *trpEGDCFBA* transcriptional unit, of which *trpBA* encode the subunits of tryptophan synthase, and *trpEGDCF*, encode enzymes necessary for synthesis of indole precursor. *Chlamydia trachomatis* uniformly lack the genes needed to produce indole, but strains that cause ocular vs. genital infections can be differentiated on the basis of the latter being able to produce a functional tryptophan synthase, and it is postulated that tryptophan can be produced by condensation of serine with exogenous indole produced by microflora in the female genital tract (Fehlner-Gardiner et al., 2002; McClarty et al., 2007). Consequently, tryptophan auxotrophy may contribute to tropism of TSST producing CC30 strains for the vaginal mucosa.

Another important factor in evolution of niche adapted strains is an increase in copy number of IS elements, leading to genome deletions and inversions through recombination between adjacent IS elements. An interesting example relevant to our analysis

is a reduction in the numbers of operons encoding 16S-23S rRNA in microbial endosymbionts of insect cells (Andersson and Andersson, 1999; Itoh et al., 2002). This was attributed to IS integration within operons encoding 16S-23S rRNA, followed by recombination to generate deletions (Dale et al., 2003). It is, therefore, striking that all three 16S-23S-5S rRNA loci in the CC30 genome are targeted by ISSau2, with an insertion at rRNA-3 being unique to Clade 1, while insertions at rRNA-1 and rRNA-2 are unique to HA-MRSA in Clade 3 (**Figure 1** and **Table 2**). Our analysis suggests that the insertions adjacent to rRNA operons is due to the propensity of ISSau2 to target inverted repeats, which likely comprise *rho*-independent transcription terminators. ISSau2 is a member of the IS30 family, and two unusual members of the IS30 family in *Mycoplasma fermentans* and *M. bovis*, which are obligate intracellular parasites, also target *rho*-independent transcription terminators, which remain intact and are partially duplicated on transposition (Calcutt et al., 1999; Lysnyansky et al., 2009). Conversely, our data suggest that ISSau2 either disrupts or weakens stem loop structures, as illustrated in **Figures 3D–G**.

Depending on the orientation of ISSau2 with respect to the adjacent gene, this could have important consequences with respect to control of transposition. It is widely accepted that transposition must be maintained at a low level, a commonly cited reason being that excessive transposition is detrimental to the stability of the host genome (Doolittle et al., 1984). Therefore, endogenous transposase promoters are generally weak, and often partially located in the inverted flanking repeats, such that strong promoters can only be created by juxtaposition of inverted repeats due to formation of head-to tail dimers, or circular copies of the IS as noted for the IS30 family (Dalrymple, 1987). IS elements also have mechanisms to attenuate their activation by impinging transcription, following insertion into active host genes. Impinging transcription across the inverted flanking repeats can either sequester translation initiation signals, or disrupt complex formation between the transposase and inverted repeats. These considerations may help to explain the insertion of ISSau2 adjacent to highly transcribed genes, including all three rRNA operons in the CC30 genome, and adjacent to *rplQ* encoding the 50S ribosomal subunit protein L17 (**Figures 1** and **3**). In these situations, ISSau2 is oriented in the antisense orientation with respect to the adjacent gene, such that impinging transcription would also generate antisense RNA to the transposase genes.

In an example that is unique to HA-MRSA in Clade 3 (**Figure 1** and **Table 2**), ISSau2 is inserted in the sense orientation adjacent to *sbcDC* (**Figure 3F**), disrupting the predicted transcriptional terminator. The *sbcDC* genes encode a protein complex that recognizes and cleaves hairpin structures in DNA, has a major role in promoting genome stability and repair of breaks in double stranded DNA, and is induced by the SOS stress response in *S. aureus* (Connelly et al., 1998; Mascarenhas et al., 2006; Chen et al., 2007; Eykelenboom et al., 2008; Darmon et al., 2010). It is noteworthy in this respect that loss of DNA recombinational repair occurs in the initial stages of genome degeneration, as bacteria undergo a transition from an autonomous free-living state to permanent intracellular existence (Dale et al., 2003). This leads to active expansion of IS elements, which in turn promotes deletion or inversion of genome segments *via* IS-mediated recombination. Therefore, based on established evolutionary trends, the ISSau2 insertion adjacent to *sbcDC* may represent an early stage in the pathway toward genome destabilization.

Whether ISSau2 influences expression of adjacent genes is unknown. However, an insertion that is unique to strain MN8, from a case of menstrual Staphylococcal toxic shock, is adjacent to the *saeRS* two-component sensory signal transducer. SaeRS is a major regulator of virulence in *S. aureus* (Geiger et al., 2008; Voyich et al., 2009; Nygaard et al., 2010), and although there is as yet no evidence that ISSau2 influences expression of *saeRS*, we find that relative to ST30*spa33* strains that lack this insertion, MN8 exhibits more abundant production of secreted proteins, including the HglA, HglB, and HglC components of γ-hemolysin, as well as TSST and SAR0385 gene product encoded on SaPI2 and SaPI4, respectively. This is consistent with a recent finding that, with the exception of strain MN8, other ST30*spa33* strains and EMRSA-16 exhibited strongly attenuated transcription of the RNAIII effector component of the *agr* global regulator, due to a common SNP in *agrC* (DeLeo et al., 2011). Although this SNP is also present in strain MN8, transcription of RNAIII was not influenced to the same extent as other strains, suggesting that there was a compensatory mechanism in this strain. Additional work is warranted to determine if this is related to the ISSau2 insertion adjacent to *saeRS*.

The absence of the *yefM-yoeB* TA module (*toxM*) in Clade 3 is also consistent with established evolutionary pathways toward niche adaptation. Most free-living bacteria have multiple genomic TA loci, which are thought to help cope with nutritional stress by inducing a reversible state of dormancy during periods of nutrient depletion (Pedersen et al., 2002; Gerdes et al., 2005), although this has been disputed in *E. coli* (Tsilibaris et al., 2007). However, obligate intracellular pathogens and symbionts experience a less variable environment, and do not have TA modules (Pandey and Gerdes, 2005). Only a few free-living bacteria lack TA modules, the most notable being *Lactococcus lactis*, which is niche-adapted in its association with dairy products. Intriguingly, outside of CC30, the only other *S. aureus* genomes that lack this TA module thus far are restricted to ST398 porcine adapted *S. aureus*, ovine adapted strains 011 and 046, and as yet undefined strains A9635 and 21200. Although we cannot exclude the possibility that this TA module represents a gene acquisition in Clades 1 and 2, rather than a gene deletion in Clade 3, the broad distribution of this element in other *S. aureus* genomes supports the contention that this element is a component of the core genome that is lost in evolutionary development of some strains. However, more work is needed to confirm this hypothesis.

In conclusion, our findings support the notion that Clade 3 is following an evolutionary blueprint toward niche-adaptation, while Clade 2 strains consisting of ST30*spa19* CA-MRSA retain the feral nature of the historic PT80/81 Clade 1. It is important to note that CA-MRSA are defined by Type IV SCC*mec*, which in CC30 is also associated with ST30*spa*43 and ST30*spa*16 strains in Clade 3 (**Table 2**). Therefore, strains of CA-MRSA, which are typically associated with hyper-virulence, are emerging with the niche-adapted trait. Given that CA-MRSA must evolve from MSSA through acquisition of Type IV SCC*mec*, this suggests that the niche-adapted trait is widely disseminated in the human

population, and this is supported by several key observations. First, MSSA that resemble the EMRSA-16 clone of HA-MRSA (Clade 3) were the most common clonal type associated with asymptomatic nasal carriage in the United States (Kuehnert et al., 2006), and several other studies concur that CC30 is a major clonal complex associated with nasal carriage (Feil et al., 2003; Melles et al., 2004, 2008; Kuehnert et al., 2006; Fowler et al., 2007; Ko et al., 2008). Second, *S. aureus* infections are usually caused by the same strain that is associated with nasal carriage, and in our analysis of a panel of 172 CC30 clinical isolates, the occurrence of the *hla* pseudogene, the *agrC* SNP, and *tst* encoded by SaPI2, which are key markers of Clade 3 (**Table 2**), was 70.9%, 72.1%, and 75.6%, respectively, (DeLeo et al., 2011). Third, in a study that assessed nasal carriage isolates from 107 healthy blood donors, 27% were CC30, and 62% of these CC30 strains possessed *tst* (Holtfreter et al., 2007), which is a marker of Clade 3. Moreover, in the same study, *tst* was present in 90% of CC30 bacteremia isolates. In this context, although our studies indicate that the niche adapted trait is associated with attenuated virulence in murine infection models (Holtfreter et al., 2007), a benefit to Clade 3 in having premature stop codons in Hla and IsdH (**Table 2**) is that both proteins are considered as potential vaccine antigens (Clarke et al., 2006; Wardenburg and Schneewind, 2008; Kennedy et al., 2010; Ster et al., 2010), and Clade 3 strains would be immune to this vaccine strategy.

ACKNOWLEDGMENTS

This research was supported by a grant to Martin J. McGavin from the Natural Sciences and Engineering Research Council of Canada.

REFERENCES

Abbott, A. (2005). Medics braced for fresh superbug. *Nature* 436, 758.

Altemeier, W. A., Lewis, S., Schlievert, P. M., and Bjornson, H. S. (1981). Studies of the Staphylococcal causation of toxic shock syndrome. *Surg. Gynecol. Obstet.* 153, 481–485.

Andersson, J. O., and Andersson, S. G. (1999). Insights into the evolutionary process of genome degradation. *Curr. Opin. Genet. Dev.* 9, 664–671.

Baba, T., Takeuchi, F., Kuroda, M., Yuzawa, H., Aoki, K., Oguchi, A., Nagai, Y., Iwama, N., Asano, K., Naimi, T., Kuroda, H., Cui, L., Yamamoto, K., and Hiramatsu, K. (2002). Genome and virulence determinants of high virulence community-acquired MRSA. *Lancet* 359, 1819–1827.

Brazier, J. S. (2008). *Clostridium difficile*: from obscurity to superbug. *Br. J. Biomed. Sci.* 65, 39–44.

Bubeck Wardenburg, J., Bae, T., Otto, M., Deleo, F. R., and Schneewind, O. (2007). Poring over pores: alpha-hemolysin and Panton-Valentine leukocidin in *Staphylococcus aureus* pneumonia. *Nat. Med.* 13, 1405–1406.

Calcutt, M. J., Lavrrar, J. L., and Wise, K. S. (1999). IS1630 of *Mycoplasma fermentans*, a novel IS30-type insertion element that targets and duplicates inverted repeats of variable length and sequence during insertion. *J. Bacteriol.* 181, 7597–7607.

Cassat, J. E., Dunman, P. M., McAleese, F., Murphy, E., Projan, S. J., and Smeltzer, M. S. (2005). Comparative genomics of *Staphylococcus aureus* Musculoskeletal isolates. *J. Bacteriol.* 187, 576–592.

Charpentier, E., Anton, A. I., Barry, P., Alfonso, B., Fang, Y., and Novick, R. P. (2004). Novel cassette-based shuttle vector system for Gram-positive bacteria. *Appl. Environ. Microbiol.* 70, 6076–6085.

Chen, Z., Luong, T. T., and Lee, C. Y. (2007). The *sbcDC* locus mediates repression of type 5 capsule production as part of the SOS response in *Staphylococcus aureus*. *J. Bacteriol.* 189, 7343–7350.

Chu, M. C., Melish, M. E., and James, J. F. (1985). Tryptophan auxotypy associated with *Staphylococcus aureus* that produce toxic-shock-syndrome toxin. *J. Infect. Dis.* 151, 1157–1158.

Clarke, S. R., Brummell, K. J., Horsburgh, M. J., McDowell, P. W., Mohamad, S. A., Stapleton, M. R., Acevedo, J., Read, R. C., Day, N. P., Peacock, S. J., Mond, J. J., Kokai-Kun, J. F., and Foster, S. J. (2006). Identification of in vivo-expressed antigens of *Staphylococcus aureus* and their use in vaccinations for protection against nasal carriage. *J. Infect. Dis.* 193, 1098–1108.

Connelly, J. C., Kirkham, L. A., and Leach, D. R. (1998). The SbcCD nuclease of *Escherichia coli* is a structural maintenance of chromosomes (SMC) family protein that cleaves hairpin DNA. *Proc. Natl. Acad. Sci. U.S.A.* 95, 7969–7974.

Cox, R. A., Conquest, C., Mallaghan, C., and Marples, R. R. (1995). A major outbreak of methicillin-resistant *Staphylococcus aureus* caused by a new phage-type (EMRSA-16). *J. Hosp. Infect.* 29, 87–106.

Dale, C., Wang, B., Moran, N., and Ochman, H. (2003). Loss of DNA recombinational repair enzymes in the initial stages of genome degeneration. *Mol. Biol. Evol.* 20, 1188–1194.

Dalrymple, B. (1987). Novel rearrangements of IS30 carrying plasmids leading to the reactivation of gene expression. *Mol. Gen. Genet.* 207, 413–420.

Darmon, E., Eykelenboom, J. K., Lincker, F., Jones, L. H., White, M., Okely, E., Blackwood, J. K., and Leach, D. R. (2010). *E. coli* SbcCD and RecA control chromosomal rearrangement induced by an interrupted palindrome. *Mol. Cell* 39, 59–70.

DeLeo, F. R., Kennedy, A. D., Chen, L., Bubeck Wardenburg, J., Kobayashi, S. D., Mathema, B., Braughton, K. R., Whitney, A. R., Villaruz, A. E., Martens, C. A., Porcella, S. F., McGavin, M. J., Otto, M., Musser, J. M., and Kreiswirth, B. N. (2011). Molecular differentiation of historic phage-type 80/81 and contemporary epidemic *Staphylococcus aureus*. *Proc. Natl. Acad. Sci. U.S.A.* 108, 18091–18096.

Delorme, C., Godon, J. J., Ehrlich, S. D., and Renault, P. (1993). Gene inactivation in *Lactococcus lactis*: histidine biosynthesis. *J. Bacteriol.* 175, 4391–4399.

Doolittle, W. F., Kirkwood, T. B., and Dempster, M. A. (1984). Selfish DNAs with self-restraint. *Nature* 307, 501–502.

Enright, M. C., Day, N. P., Davies, C. E., Peacock, S. J., and Spratt, B. G. (2000). Multilocus sequence typing for characterization of methicillin-resistant and methicillin-susceptible clones of *Staphylococcus aureus*. *J. Clin. Microbiol.* 38, 1008–1015.

Eykelenboom, J. K., Blackwood, J. K., Okely, E., and Leach, D. R. (2008). SbcCD causes a double-strand break at a DNA palindrome in the *Escherichia coli* chromosome. *Mol. Cell* 29, 644–651.

Fehlner-Gardiner, C., Roshick, C., Carlson, J. H., Hughes, S., Belland, R. J., Caldwell, H. D., and McClarty, G. (2002). Molecular basis defining human *Chlamydia trachomatis* tissue tropism. A possible role for tryptophan synthase. *J. Biol. Chem.* 277, 26893–26903.

Feil, E. J., Cooper, J. E., Grundmann, H., Robinson, D. A., Enright, M. C., Berendt, T., Peacock, S. J., Smith, J. M., Murphy, M., Spratt, B. G., Moore, C. E., and Day, N. P. (2003). How clonal is *Staphylococcus aureus*? *J. Bacteriol.* 185, 3307–3316.

Foster, T. J. (2004). The *Staphylococcus aureus* "superbug". *J. Clin. Invest.* 114, 1693–1696.

Fowler, V. G. Jr., Nelson, C. L., McIntyre, L. M., Kreiswirth, B. N., Monk, A., Archer, G. L., Federspiel, J., Naidich, S., Remortel, B., Rude, T., Brown, P., Reller, L. B., Corey, G. R., and Gill, S. R. (2007). Potential associations between hematogenous complications and bacterial genotype in *Staphylococcus aureus* infection. *J. Infect. Dis.* 196, 738–747.

Fu, Z., Donegan, N. P., Memmi, G., and Cheung, A. L. (2007). Characterization of MazFSa, an endoribonuclease from *Staphylococcus aureus*. *J. Bacteriol.* 189, 8871–8879.

Garcia-Alvarez, L., Holden, M. T., Lindsay, H., Webb, C. R., Brown, D. F., Curran, M. D., Walpole, E., Brooks, K., Pickard, D. J., Teale, C., Parkhill, J., Bentley, S. D., Edwards, G. F., Girvan, E. K., Kearns, A. M., Pichon, B., Hill, R. L., Larsen, A. R., Skov, R. L., Peacock, S. J., Maskell, D. J., and Holmes, M. A. (2011). Meticillin-resistant *Staphylococcus aureus* with a novel *mecA* homologue in human and bovine populations in the UK and Denmark: a descriptive study. *Lancet Infect. Dis.* 11, 595–603.

Geiger, T., Goerke, C., Mainiero, M., Kraus, D., and Wolz, C. (2008). The virulence regulator

Sae of *Staphylococcus aureus*: promoter activities and response to phagocytosis-related signals. *J. Bacteriol.* 190, 3419–3428.

Gerdes, K., Christensen, S. K., and Lobner-Olesen, A. (2005). Prokaryotic toxin-antitoxin stress response loci. *Nat. Rev. Microbiol.* 3, 371–382.

Gillaspy, A. F., Hickmon, S. G., Skinner, R. A., Thomas, J. R., Nelson, C. L., and Smeltzer, M. S. (1995). Role of the accessory gene regulator (*agr*) in pathogenesis of *Staphylococcal osteomyelitis*. *Infect. Immun.* 63, 3373–3380.

Guinane, C. M., Ben Zakour, N. L., Tormo-Mas, M. A., Weinert, L. A., Lowder, B. V., Cartwright, R. A., Smyth, D. S., Smyth, C. J., Lindsay, J. A., Gould, K. A., Witney, A., Hinds, J., Bollback, J. P., Rambaut, A., Penades, J. R., and Fitzgerald, J. R. (2010). Evolutionary genomics of *Staphylococcus aureus* reveals insights into the origin and molecular basis of ruminant host adaptation. *Genome Biol. Evol.* 2, 454–466.

Guo, Y., Wang, J., Niu, G., Shui, W., Sun, Y., Zhou, H., Zhang, Y., Yang, C., Lou, Z., and Rao, Z. (2011). A structural view of the antibiotic degradation enzyme NDM-1 from a superbug. *Protein Cell* 2, 384–394.

Gyenis, L., Duncan, J. S., Turowec, J. P., Bretner, M., and Litchfield, D. W. (2011). Unbiased functional proteomics strategy for protein kinase inhibitor validation and identification of bona fide protein kinase substrates: application to identification of as a substrate for CK2. *J. Proteome Res.* 10, 4887–4901.

Hassall, J. E., and Rountree, P. M. (1959). Staphylococcal septicaemia. *Lancet* 1, 213–217.

Herron-Olson, L., Fitzgerald, J. R., Musser, J. M., and Kapur, V. (2007). Molecular correlates of host Specialization in *Staphylococcus aureus*. *PLoS One* 2:e1120. doi: 10.1371/journal.pone.0001120

Holden, M. T., Feil, E. J., Lindsay, J. A., Peacock, S. J., Day, N. P., Enright, M. C., Foster, T. J., Moore, C. E., Hurst, L., Atkin, R., Barron, A., Bason, N., Bentley, S. D., Chillingworth, C., Chillingworth, T., Churcher, C., Clark, L., Corton, C., Cronin, A., Doggett, J., Dowd, L., Feltwell, T., Hance, Z., Harris, B., Hauser, H., Holroyd, S., Jagels, K., James, K. D., Lennard, N., Line, A., Mayes, R., Moule, S., Mungall, K., Ormond, D., Quail, M. A., Rabbinowitsch, E., Rutherford, K., Sanders, M., Sharp, S., Simmonds, M., Stevens, K., Whitehead, S., Barrell, B. G., Spratt, B. G., and Parkhill, J. (2004). Complete genomes of two clinical *Staphylococcus aureus* strains: evidence for the rapid evolution of virulence and drug resistance. *Proc. Natl. Acad. Sci. U.S.A.* 101, 9786–9791.

Holtfreter, S., Grumann, D., Schmudde, M., Nguyen, H. T., Eichler, P., Strommenger, B., Kopron, K., Kolata, J., Giedrys-Kalemba, S., Steinmetz, I., Witte, W., and Broker, B. M. (2007). Clonal distribution of superantigen genes in clinical *Staphylococcus aureus* isolates. *J. Clin. Microbiol.* 45, 2669–2680.

Itoh, T., Martin, W., and Nei, M. (2002). Acceleration of genomic evolution caused by enhanced mutation rate in endocellular symbionts. *Proc. Natl. Acad. Sci. U.S.A.* 99, 12944–12948.

Johnson, A. P., Aucken, H. M., Cavendish, S., Ganner, M., Wale, M. C., Warner, M., Livermore, D. M., and Cookson, B. D. (2001). Dominance of EMRSA-15 and -16 among MRSA causing nosocomial bacteraemia in the UK: analysis of isolates from the European Antimicrobial Resistance Surveillance System (EARSS). *J. Antimicrob. Chemother.* 48, 143–144.

Kamada, K., and Hanaoka, F. (2005). Conformational change in the catalytic site of the ribonuclease YoeB toxin by YefM antitoxin. *Mol. Cell* 19, 497–509.

Kennedy, A. D., Bubeck Wardenburg, J., Gardner, D. J., Long, D., Whitney, A. R., Braughton, K. R., Schneewind, O., and Deleo, F. R. (2010). Targeting of alpha-hemolysin by active or passive immunization decreases severity of USA300 skin infection in a mouse model. *J. Infect. Dis.* 202, 1050–1058.

Ko, K. S., Lee, J. Y., Baek, J. Y., Peck, K. R., Rhee, J. Y., Kwon, K. T., Heo, S. T., Ahn, K. M., and Song, J. H. (2008). Characterization of *Staphylococcus aureus* nasal carriage from children attending an outpatient clinic in Seoul, Korea. *Microb. Drug Resist.* 14, 37–44.

Kreiswirth, B. N., Projan, S. J., Schlievert, P. M., and Novick, R. P. (1989). Toxic shock syndrome toxin 1 is encoded by a variable genetic element. *Rev. Infect. Dis.* 11(Suppl. 1), S83–S88. discussion S88–S89.

Kuehnert, M. J., Kruszon-Moran, D., Hill, H. A., McQuillan, G., McAllister, S. K., Fosheim, G., McDougal, L. K., Chaitram, J., Jensen, B., Fridkin, S. K., Killgore, G., and Tenover, F. C. (2006). Prevalence of *Staphylococcus aureus* nasal colonization in the United States, 2001–2002. *J. Infect. Dis.* 193, 172–179.

Kuroda, M., Ohta, T., Uchiyama, I., Baba, T., Yuzawa, H., Kobayashi, I., Cui, L., Oguchi, A., Aoki, K., Nagai, Y., Lian, J., Ito, T., Kanamori, M., Matsumaru, H., Maruyama, A., Murakami, H., Hosoyama, A., Mizutani-Ui, Y., Takahashi, N. K., Sawano, T., Inoue, R., Kaito, C., Sekimizu, K., Hirakawa, H., Kuhara, S., Goto, S., Yabuzaki, J., Kanehisa, M., Yamashita, A., Oshima, K., Furuya, K., Yoshino, C., Shiba, T., Hattori, M., Ogasawara, N., Hayashi, H., and Hiramatsu, K. (2001). Whole genome sequencing of meticillin-resistant *Staphylococcus aureus*. *Lancet* 357, 1225–1240.

Kwan, T., Liu, J., Dubow, M., Gros, P., and Pelletier, J. (2005). The complete genomes and proteomes of 27 *Staphylococcus aureus* bacteriophages. *Proc. Natl. Acad. Sci. U.S.A.* 102, 5174–5179.

Le Marechal, C., Hernandez, D., Schrenzel, J., Even, S., Berkova, N., Thiery, R., Vautor, E., Fitzgerald, J. R., Francois, P., and Le Loir, Y. (2011). Genome sequences of two *Staphylococcus aureus* ovine strains that induce severe (strain O11) and mild (strain O46) mastitis. *J. Bacteriol.* 193, 2353–2354.

Leung, D. Y., Meissner, H. C., Fulton, D. R., Murray, D. L., Kotzin, B. L., and Schlievert, P. M. (1993). Toxic shock syndrome toxin-secreting *Staphylococcus aureus* in Kawasaki syndrome. *Lancet* 342, 1385–1388.

Li, Z., Stevens, D. L., Hamilton, S. M., Parimon, T., Ma, Y., Kearns, A. M., Ellis, R. W., and Bryant, A. E. (2011). Fatal *S. aureus* hemorrhagic pneumonia: genetic analysis of a unique clinical isolate producing both PVL and TSST-1. *PLoS One* 6:e27246. doi: 10.1371/journal.pone.0027246

Lin, Y. C., Anderson, M. J., Kohler, P. L., Strandberg, K. L., Olson, M. E., Horswill, A. R., Schlievert, P. M., and Peterson, M. L. (2011). Proinflammatory exoprotein characterization of toxic shock syndrome *Staphylococcus aureus*. *Biochemistry* 50, 7157–7167.

Lindsay, J. A., and Holden, M. T. (2004). *Staphylococcus aureus*: superbug, super genome? *Trends Microbiol.* 12, 378–385.

Lindsay, J. A., Ruzin, A., Ross, H. F., Kurepina, N., and Novick, R. P. (1998). The gene for toxic shock toxin is carried by a family of mobile pathogenicity islands in *Staphylococcus aureus*. *Mol. Microbiol.* 29, 527–543.

Lowder, B. V., Guinane, C. M., Ben Zakour, N. L., Weinert, L. A., Conway-Morris, A., Cartwright, R. A., Simpson, A. J., Rambaut, A., Nubel, U., and Fitzgerald, J. R. (2009). Recent human-to-poultry host jump, adaptation, and pandemic spread of *Staphylococcus aureus*. *Proc. Natl. Acad. Sci. U.S.A.* 106, 19545–19550.

Lysnyansky, I., Calcutt, M. J., Ben-Barak, I., Ron, Y., Levisohn, S., Methe, B. A., and Yogev, D. (2009). Molecular characterization of newly identified IS3, IS4 and IS30 insertion sequence-like elements in *Mycoplasma bovis* and their possible roles in genome plasticity. *FEMS Microbiol. Lett.* 294, 172–182.

Mascarenhas, J., Sanchez, H., Tadesse, S., Kidane, D., Krisnamurthy, M., Alonso, J. C., and Graumann, P. L. (2006). *Bacillus subtilis* SbcC protein plays an important role in DNA inter-strand cross-link repair. *BMC Mol. Biol.* 7, 20.

McClarty, G., Caldwell, H. D., and Nelson, D. E. (2007). *Chlamydial* interferon gamma immune evasion influences infection tropism. *Curr. Opin. Microbiol.* 10, 47–51.

McDougal, L. K., Steward, C. D., Killgore, G. E., Chaitram, J. M., McAllister, S. K., and Tenover, F. C. (2003). Pulsed-field gel electrophoresis typing of oxacillin-resistant *Staphylococcus aureus* isolates from the United States: establishing a national database. *J. Clin. Microbiol.* 41, 5113–5120.

Meinhart, A., Alonso, J. C., Strater, N., and Saenger, W. (2003). Crystal structure of the plasmid maintenance system epsilon/zeta: functional mechanism of toxin zeta and inactivation by epsilon 2 zeta 2 complex formation. *Proc. Natl. Acad. Sci. U.S.A.* 100, 1661–1666.

Melles, D. C., Gorkink, R. F., Boelens, H. A., Snijders, S. V., Peeters, J. K., Moorhouse, M. J., van der Spek, P. J., van Leeuwen, W. B., Simons, G., Verbrugh, H. A., and van Belkum, A. (2004). Natural population dynamics and expansion of pathogenic clones of *Staphylococcus aureus*. *J. Clin. Invest* 114, 1732–1740.

Melles, D. C., Tenover, F. C., Kuehnert, M. J., Witsenboer, H., Peeters, J. K., Verbrugh, H. A., and van Belkum, A. (2008). Overlapping population structures of nasal isolates of *Staphylococcus aureus* from healthy Dutch and American individuals. *J. Clin. Microbiol.* 46, 235–241.

Moore, P. C., and Lindsay, J. A. (2002). Molecular characterisation of the dominant UK methicillin-resistant *Staphylococcus aureus* strains, EMRSA-15 and EMRSA-16. *J. Med. Microbiol.* 51, 516–521.

Moran, N. A., and Plague, G. R. (2004). Genomic changes following host restriction in bacteria. *Curr. Opin. Genet. Dev.* 14, 627–633.

Nickerson, N., Ip, J., Passos, D. T., and McGavin, M. J. (2010). Comparison of Staphopain A (ScpA) and B (SspB) precursor activation mechanisms reveals unique secretion kinetics of proSspB (Staphopain B), and a different interaction with its cognate Staphostatin, SspC. *Mol. Microbiol.* 75, 161–177.

Nienaber, J. J., Sharma Kuinkel, B. K., Clarke-Pearson, M., Lamlertthon, S., Park, L., Rude, T. H., Barriere, S., Woods, C. W., Chu, V. H., Marin, M., Bukovski, S., Garcia, P., Corey, G. R., Korman, T., Doco-Lecompte, T., Murdoch, D. R., Reller, L. B., and Fowler, V. G. Jr. (2011). Methicillin-susceptible *Staphylococcus aureus* endocarditis isolates are associated with clonal complex 30 genotype and a distinct repertoire of enterotoxins and adhesins. *J. Infect. Dis.* 204, 704–713.

Novick, R. P. (1991). Genetic systems in staphylococci. *Methods Enzymol.* 204, 587–636.

Novick, R. P., and Subedi, A. (2007). The SaPIs: mobile pathogenicity islands of Staphylococcus. *Chem. Immunol. Allergy* 93, 42–57.

Nygaard, T. K., Pallister, K. B., Ruzevich, P., Griffith, S., Vuong, C., and Voyich, J. M. (2010). SaeR binds a consensus sequence within virulence gene promoters to advance USA300 pathogenesis. *J. Infect. Dis.* 201, 241–254.

Pallen, M. J., and Wren, B. W. (2007). Bacterial pathogenomics. *Nature* 449, 835–842.

Pandey, D. P., and Gerdes, K. (2005). Toxin-antitoxin loci are highly abundant in free-living but lost from host-associated prokaryotes. *Nucleic Acids Res.* 33, 966–976.

Pedersen, K., Christensen, S. K., and Gerdes, K. (2002). Rapid induction and reversal of a bacteriostatic condition by controlled expression of toxins and antitoxins. *Mol. Microbiol.* 45, 501–510.

Pilpa, R. M., Fadeev, E. A., Villareal, V. A., Wong, M. L., Phillips, M., and Clubb, R. T. (2006). Solution structure of the NEAT (NEAr Transporter) domain from IsdH/HarA: the human hemoglobin receptor in *Staphylococcus aureus*. *J. Mol. Biol.* 360, 435–447.

Prere, M. F., Chandler, M., and Fayet, O. (1990). Transposition in *Shigella dysenteriae*: isolation and analysis of IS911, a new member of the IS3 group of insertion sequences. *J. Bacteriol.* 172, 4090–4099.

Robinson, D. A., Kearns, A. M., Holmes, A., Morrison, D., Grundmann, H., Edwards, G., O'Brien, F. G., Tenover, F. C., McDougal, L. K., Monk, A. B., and Enright, M. C. (2005). Re-emergence of early pandemic *Staphylococcus aureus* as a community-acquired meticillin-resistant clone. *Lancet* 365, 1256–1258.

Rountree, P. M., and Beard, M. A. (1958). Further observations on infection with phage type 80 Staphylococci in Australia. *Med. J. Aust.* 45, 789–795.

Ruzin, A., Lindsay, J., and Novick, R. P. (2001). Molecular genetics of SaPI1–a mobile pathogenicity island in *Staphylococcus aureus*. *Mol. Microbiol.* 41, 365–377.

Schijffelen, M. J., Boel, C. H., van Strijp, J. A., and Fluit, A. C. (2010). Whole genome analysis of a livestock-associated methicillin-resistant *Staphylococcus aureus* ST398 isolate from a case of human endocarditis. *BMC Genomics* 11, 376.

Schlievert, P. M., and Blomster, D. A. (1983). Production of Staphylococcal pyrogenic exotoxin type C: influence of physical and chemical factors. *J. Infect. Dis.* 147, 236–242.

Sekine, Y., Eisaki, N., and Ohtsubo, E. (1994). Translational control in production of transposase and in transposition of insertion sequence IS3. *J. Mol. Biol.* 235, 1406–1420.

Sekine, Y., Izumi, K., Mizuno, T., and Ohtsubo, E. (1997). Inhibition of transpositional recombination by OrfA and OrfB proteins encoded by insertion sequence IS3. *Genes Cells* 2, 547–557.

Seybold, U., Kourbatova, E. V., Johnson, J. G., Halvosa, S. J., Wang, Y. F., King, M. D., Ray, S. M., and Blumberg, H. M. (2006). Emergence of community-associated methicillin-resistant *Staphylococcus aureus* USA300 genotype as a major cause of health care-associated blood stream infections. *Clin. Infect. Dis.* 42, 647–656.

Shopsin, B., Gomez, M., Montgomery, S. O., Smith, D. H., Waddington, M., Dodge, D. E., Bost, D. A., Riehman, M., Naidich, S., and Kreiswirth, B. N. (1999). Evaluation of protein A gene polymorphic region DNA sequencing for typing of *Staphylococcus aureus* strains. *J. Clin. Microbiol.* 37, 3556–3563.

Ster, C., Beaudoin, F., Diarra, M. S., Jacques, M., Malouin, F., and Lacasse, P. (2010). Evaluation of some *Staphylococcus aureus* iron-regulated proteins as vaccine targets. *Vet. Immunol. Immunopathol.* 136, 311–318.

Tanimoto, R. H. (1962). Observations on *Staphylococcus aureus* phage-type 80/81 Hawaii and its resistance to antibiotics. *Hawaii Med. J.* 21, 262–265.

Timmerman, K. P., and Tu, C. P. (1985). Complete sequence of IS3. *Nucleic Acids Res.* 13, 2127–2139.

Tsilibaris, V., Maenhaut-Michel, G., Mine, N., and van Melderen, L. (2007). What is the benefit to *Escherichia coli* of having multiple toxin-antitoxin systems in its genome? *J. Bacteriol.* 189, 6101–6108.

Voyich, J. M., Vuong, C., Dewald, M., Nygaard, T. K., Kocianova, S., Griffith, S., Jones, J., Iverson, C., Sturdevant, D. E., Braughton, K. R., Whitney, A. R., Otto, M., and Deleo, F. R. (2009). The SaeR/S gene regulatory system is essential for innate immune evasion by *Staphylococcus aureus*. *J. Infect. Dis.* 199, 1698–1706.

Wardenburg, J. B., and Schneewind, O. (2008). Vaccine protection against *Staphylococcus aureus* pneumonia. *J. Exp. Med.* 205, 287–294.

Williams, J. R., Talbot, E. C., and Maughan, E. (1959). Hospital outbreak of cross-infection due to *Staphylococcus pyogenes* phage type 80. *Br. Med. J.* 1, 1374–1378.

Wormald, P. J. (1961). Multiple endemic substrains of *Staphylococcus pyogenes* phage type 80. *Monatsschr. Unfallheilkd. Versicherungsmed.* 20, 59–62.

Xiong, Y. Q., Fowler, V. G., Yeaman, M. R., Perdreau-Remington, F., Kreiswirth, B. N., and Bayer, A. S. (2009). Phenotypic and genotypic characteristics of persistent methicillin-resistant *Staphylococcus aureus* bacteremia *in vitro* and in an experimental endocarditis model. *J. Infect. Dis.* 199, 201–208.

Conflict of Interest Statement: The authors declare that the research was conducted in the absence of any commercial or financial relationships that could be construed as a potential conflict of interest.

Received: 23 January 2012; accepted: 20 March 2012; published online: 09 April 2012.

Citation: McGavin MJ, Arsic B and Nickerson NN (2012) Evolutionary blueprint for host- and niche-adaptation in Staphylococcus aureus clonal complex CC30. Front. Cell. Inf. Microbio. ***2****:48. doi: 10.3389/fcimb.2012.00048*